NIH Public Access
Author Manuscript
J Cardiovasc Comput Tomogr. Author manuscript; available in PMC 2014 August 07.

Published in final edited form as:
J Cardiovasc Comput Tomogr. 2013 ; 7(1): 51–57. doi:10.1016/j.jcct.2012.10.010.

3D left ventricular extracellular volume fraction by low-radiation dose cardiac CT: Assessment of interstitial myocardial fibrosis

Marcelo Souto Nacif, MD, PhD[a,b,c], **Yixun Liu, PhD**[a], **Jianhua Yao, PhD**[a], **Songtao Liu, MD**[a,d], **Christopher T. Sibley, MD**[a,d], **Ronald M. Summers, MD**[a], and **David A. Bluemke, MD, PhD**[a,d,*]

[a]Radiology and Imaging Sciences, National Institutes of Health Clinical Center, Bethesda, MD, USA

[b]Division of Cardiology, Johns Hopkins University School of Medicine, Baltimore, MD, USA

[c]Radiology Department, Universidade Federal Fluminense, Niterói, Brazil

[d]National Institute of Biomedical Imaging and Bioengineering, Bethesda, MD, USA

Abstract

Background—Myocardial fibrosis leads to impaired cardiac function and events. Extracellular volume fraction (ECV) assessed with an iodinated contrast agent and measured by cardiac CT may be a useful noninvasive marker of fibrosis.

Objective—The purpose of this study was to develop and evaluate a 3-dimensional (3D) ECV calculation toolkit (ECVTK) for ECV determination by cardiac CT.

Methods—Twenty-four subjects (10 systolic heart failure, age, 60 ± 17 years; 5 diastolic failure, age 56 ± 20 years; 9 matched healthy subjects, age 59 ± 7 years) were evaluated. Cardiac CT examinations were done on a 320-multidetector CT scanner before and after 130 mL of iopamidol (Isovue-370; Bracco Diagnostics, Plainsboro, NJ, USA) was administered. A calcium score type sequence was performed before and 7 minutes after contrast with single gantry rotation during 1 breath hold and single cardiac phase acquisition. ECV was calculated as $(\Delta HU_{myocardium}/\Delta HU_{blood}) \times (1 - Hct)$ where Hct is the hematocrit, and ΔHU is the change in Hounsfield unit attenuation = $HU_{after\ iodine} - HU_{before\ iodine}$. Cardiac magnetic resonance imaging was performed to assess myocardial structure and function.

Results—Mean 3D ECV values were significantly higher in the subjects with systolic heart failure than in healthy subjects and subjects with diastolic heart failure (mean, 41% ± 6%, 33% ± 2%, and 35% ± 5%, respectively; $P = 0.02$). Interobserver and intraobserver agreements were excellent for myocardial, blood pool, and ECV (intraclass correlation coefficient, >0.90 for all). Higher 3D ECV by cardiac CT was associated with reduced systolic circumferential strain, greater end-diastolic and -systolic volumes, and lower ejection fraction ($r = 0.70$, $r = 0.60$, $r = 0.73$, and $r = -0.68$, respectively; all $P < 0.001$).

© 2013 Published by Elsevier Inc. on behalf of Society of Cardiovascular Computed Tomography.

*Corresponding author. bluemked@nih.gov (D.A. Bluemke).

Conflict of interest: The authors report no conflicts of interest.

NIH-PA Author Manuscript
NIH-PA Author Manuscript
NIH-PA Author Manuscript

NIH-PA Author Manuscript

NIH-PA Author Manuscript

NIH-PA Author Manuscript

Conclusion—3D ECV by cardiac CT can be performed with ECVTK. We demonstrated increased ECV in subjects with systolic heart failure compared with healthy subjects. Cardiac CT results also showed good correlation with important functional heart biomarkers, suggesting the potential for myocardial tissue characterization with the use of 3D ECV by cardiac CT. This trial is registered at www.ClinicalTrials.gov as NCT01160471.

Keywords

Cardiac computed tomography; Diffuse myocardial fibrosis; 3D extracellular volume

1. Introduction

Diffuse myocardial fibrosis is a common end point of a variety of cardiac risk factors and conditions, including diabetes, hypertension, hypertrophy, and even aging.[1] Myocardial extracellular volume fraction (ECV) is increased when fibrosis is present and may be a useful noninvasive marker of fibrosis.[2,3] The utility of ECV has been studied by gadolinium-enhanced cardiac magnetic resonance (MR) and involved blood pool and myocardial relaxivity before and after gadolinium quantitative T1 mapping.[2,4–6]

Cardiac CT has been validated for detection of focal myocardial scar[7–9] and myocardial perfusion.[10,11] Quantitative cardiac CT may similarly be used to map the iodine distribution in the myocardium. We have previously explored derivation of myocardial ECV on cardiac CT as a marker of interstitial fibrosis with the use of a 2-dimensional (2D) slice by slice approach,[12] showing good correlation with magnetic resonance imaging (MRI) results. That CT approach involved manual segmentation of only the lateral wall of the left ventricle on a single slice or few slices, because of difficulty in identifying blood pool versus ventricle on noncontrast CT.

We have developed a computational framework for ECV estimation[13] on CT consisting of the following 3 steps: (1) myocardium segmentation according to shape-constrained graph cut (GC) method, (2) cardiac image registration before and after contrast according to a symmetric Demons algorithm, and (3) ECV value computation. This method was tested, and the preliminary results showed the feasibility and efficiency of the proposed method. However, image processing/registration of CT before and after contrast remains an obstacle because of the need for operator intervention and long processing times.

Cardiac CT data are inherently 3 dimensional, and a 3-dimensional (3D) approach to whole-heart ECV derivation would likely improve ECV estimates. Further, whole-heart methods are generally not available for cardiac MRI. In this study, we present our results for the development of a 3D ECV calculation toolkit (ECVTK) to facilitate myocardium segmentation, CT registration before and after contrast, model generation, ECV calculation, and visualization. Our experiments indicate that ECVTK was more effective in improving the CT accuracy in comparison with our previous GC method.[13,14] Thus, this may produce a more efficient and user-friendly method for 3D ECV calculations. The purpose of this study was to develop and evaluate a 3D approach to determine ECV with the use of cardiac CT.

NIH-PA Author Manuscript

NIH-PA Author Manuscript

NIH-PA Author Manuscript

2. Methods

2.1. Study population

This study was approved by our institutional review board. All study participants provided written informed consent and completed both cardiac CT and cardiac MR studies at the same day within a 4-hour time window. From August 2010 to April 2012, 40 participants were enrolled. Patients with heart failure according to the New York Heart Association classification II or greater and either (1) left ventricular ejection fraction (LVEF) <40% or (2) evidence of elevated LV diastolic filling pressure and LVEF >50% were included as well as healthy persons for comparison, thus providing a wide range of ECV values. Healthy volunteers had no history of clinical cardiovascular disease, including myocardial infarction, heart failure, coronary artery disease, sudden cardiac death, or valvular heart disease.

Normal LV and right ventricular volumes and systolic functions were confirmed by cardiac MR as part of the routine study. Steady-state free-precession cine-MR short-axis images were acquired with temporal resolution of 40 milliseconds to assess LV function. Fast gradient echo images with the use of spatial modulation of magnetization (tagged MRI) was obtained for strain analysis.[15] Phase sensitive inversion recovery late gadolinium enhancement imaging was obtained at 15 minutes after injection to assess for focal myocardial scar. Inversion times were individually adjusted to suppress normal myocardium.[16]

Subjects with contraindications to cardiac MR or cardiac CT, including contrast reaction and glomerular filtration rate <30 mL/min/1.73m^2 were excluded. All clinical examinations and laboratory tests presented were evaluated no more than 7 days before the cardiac CT study.

2.2. Cardiac CT protocol

All study participants were imaged on a 320-multidetector CT scanner (Aquilion One; Toshiba Medical Systems, Tustin, CA, USA) after the cardiac MR examination. A calcium score type acquisition before contrast was performed with the use of prospective electrocardiogram (ECG) gating with a 400-millisecond single gantry rotation during inspiration breath hold that allows image acquisition at a single cardiac phase. Scan parameters were tube voltage of 120 kV, tube current of 300 mA, and slice thickness of 0.5 mm (reconstructed for 3 mm).[17] Coronary CT angiography was performed during intravenous infusion of 133 ± 16 mL of iopamidol (Isovue-370; Bracco Diagnostics, Plainsboro, NJ, USA) at a rate of 4–5 mL/s with the use of the following parameters: for heart rate <66 beats/min, prospective ECG gating at 70%–80% of 1 R–R interval, x-ray exposure time ranges from 0.423 to 0.350 second. For heart rate ≥66 beats/min, prospective ECG gating at 40%–80% of 2 R–R intervals, x-ray exposure time ranges from 1.174 seconds to 0.714 second. Additional parameters were tube voltage of 120 kV; tube current of 300–580 mA, depending on body mass index (BMI; calculated as weight in kg/height in m^2) and sex; gantry rotation speed of 0.35 second; slice thickness of 0.5 mm; and scan range of 128–160 mm.

After a 7- to 10-minute delay, a cardiac CT scan after contrast was acquired with identical parameters as the coronary calcium scan before contrast. Radiation dose estimation was

NIH-PA Author Manuscript

NIH-PA Author Manuscript

NIH-PA Author Manuscript

based on the dose length product provided by the scanner for each patient and by using the correction factor 0.014 for chest imaging in adults.[18]

2.3. 3D ECV calculation toolkit

An ECVTK was developed by integrating myocardium segmentation, before and after contrast CT registration, model generation, ECV calculation, and visualization into a unified framework to facilitate the assessment of interstitial myocardial fibrosis with the use of ECV. Myocardium segmentation performed on the low-dose CT images after contrast is based on a cutting-edge model-guided segmentation method developed in our group.[14] Briefly, interlaced Bézier contours were created along both longitude and latitude directions by few guide points. The intersection points of these Bézier contours are first connected to constitute quadrilateral and triangular elements, and then each quadrilateral element is further divided into 2 triangles to produce a triangular mesh. This procedure is performed on both endocardium (endo) and epicardium (epi) to produce endo and epi surface models, and then these 2 meshes are combined into 1 closed myocardial surface model. The myocardial model has an energy function, and it includes 2 main steps: patient-specific modeling and a deformable model-based segmentation. Image registration module aligns the CT after contrast with the CT before contrast to map the myocardium in the CT before contrast. Image registration modules includes 2 submodules: point-based rigid registration and free-from deformation–based nonrigid registration. Mutual information is used as the metric of the nonrigid registration to address the change of the intensity within myocardium in the CT after contrast. Visualization module has a 3D rendering window and three 2D rendering windows. Both image data and geometry data can be visualized simultaneously in these 4 windows. To make this toolkit robust against poor-quality CT images, both myocardial contour and surface are editable to provide a backup in case the automatic segmentation method fails (Fig. 1).

2.4. Data analysis

LV end-diastolic volume (EDV) and end-systolic volume (ESV), mass, and EF were evaluated with semiautomatic 3D model-based software (CIM 6.2; MRI Research Group, University of Auckland, New Zealand).[19] Diastolic volume recovery was calculated as the time (in milliseconds) from end-systole to 80% recovery of EDV. Peak filling rate (PFR) and time to PFR were taken as the slope of the diastolic filling curve and the corresponding delay time after the end-systole phase (in mL/s). Myocardial strain was quantified with the HARP software (Diagnosoft, Palo Alto, CA, USA). Circumferential strain (peak Ecc) from basal, midcavity, and apical short-axis acquisitions were averaged.[20] By convention, Ecc is negative; less negative values indicate reduced shortening and therefore indicate worse function. Myocardial scar was defined as visually present or absent on 15-minute delayed cardiac MR.

Two observers (Y.L. and M.S.N.), who were blinded to the clinical data, qualitatively evaluated cardiac CT data with the use of the 3D approach for ECV calculation.[14] Myocardial and blood pool attenuation values were extracted from the region inside the myocardial model after the findings of the CT performed after contrast was well registered with the findings of the CT performed before contrast. The average value was used for

NIH-PA Author Manuscript

NIH-PA Author Manuscript

NIH-PA Author Manuscript

analysis (Fig. 2). ECV was calculated as (ΔHUmyocardium/ΔHUblood) × (1 − Hct) where Hct is the hematocrit, and ΔHU is the change in Hounsfield unit attenuation = $HU_{after\ iodine} - HU_{before\ iodine}$. Coronary calcium was quantified with the Agatston method.[21] Coronary calcium and CT angiogram data were analyzed with Vitrea Core fX v6 (Vital Images, Minnetonka, MN, USA).

2.5. Statistical analysis

Statistical analysis was performed with STATA, version 12.0 (StataCorp LP, College Station, TX, USA). A P value <0.05 was considered significant. Data are presented as means ± SDs for continuous variables and as percentages for categorical variables. Multiple comparisons were tested by 1-way analysis of variance with post hoc Bonferroni correction. Intraobserver and interobserver agreement were accessed with using intraclass correlation coefficient (ICC) with 2-way random model (ICC < 0.40 = poor agreement; ICC ≥ 0.40 to 0.75 = fair-to-good agreement; ICC > 0.75 = excellent agreement). The relation between clinical and imaging parameters and 3D ECV values was determined with linear or logistic regression as appropriate. Because of skewed distribution, coronary calcium was treated as log (Agatston score +1).

3. Results

A total of 24 participants were included for analysis (10 systolic heart failure, age 60 ± 17 years; 5 diastolic failure, age 56 ± 20 years; 9 matched healthy subjects, age 59 ± 7 years). Seven participants were excluded because of cardiac trigger error due to atrial fibrillation and left bundle branch block, 5 because of chest motion from shortness of breath, and 4 because of CT improper image acquisition. EF was lower in the systolic heart failure group than in healthy subjects and patients with diastolic failure (31% ± 6%, 63% ± 6%, and 60% ± 12%, respectively; $P < 0.01$). The average radiation dose was 1.98 ± 0.16 mSv each for baseline and delayed ECV measurement. Participant characteristics are summarized in Table 1.

Mean 3D ECV values were significantly higher in the subjects with systolic heart failure than in healthy subjects and subjects with diastolic heart failure (mean, 41% ± 6% vs 33% ± 2% and 35% ± 5%, respectively; $P = 0.02$; Fig. 3). These changes between groups were not otherwise detectable when only considering density differences on myocardium before contrast or myocardium after contrast ($P > 0.05$; Table 2).

For cardiac CT, interobserver and intraobserver agreements were excellent for myocardial (ICC = 0.95 and ICC = 0.97, respectively) and blood pool (ICC = 0.98 for both) attenuation measurements. Similarly for ECV, excellent agreement was found (0.94 and 0.95, respectively).

EDV and ESV and peak systolic Ecc were positively associated with 3D ECV by cardiac CT ($r = 0.60$, $r = 0.73$, and $r = 0.70$, $P < 0.001$ for all), whereas EF was inversely correlated with ECV by cardiac CT ($r = -0.68$, $P < 0.001$). No correlation was observed between Agatston score and ECV values. ECV was also unrelated to sex or age or any other clinical and imaging parameters assessed in this study (Table 3).

NIH-PA Author Manuscript

NIH-PA Author Manuscript

NIH-PA Author Manuscript

4. Discussion

Techniques for both cardiac MR and cardiac CT have been developed to identify *focal* myocardial scar due to myocardial infarction/fibrosis. Recently, innovations in cardiac MR technique have allowed assessment of *diffuse* myocardial fibrosis associated with heart failure or cardiomyopathy. In this study, we sought to derive a 3D approach that assesses the entire left ventricle for ECV calculation. With the use of a method with relatively low radiation dose, interreader and intrareader correlations for 3D ECV by cardiac CT was excellent. As expected from cardiac MR studies, ECV values were elevated in subjects with systolic heart failure, and greater ECV values were associated with reduced EF, increased ESV and EDV as well as worse Ecc.

ECV has been shown as a reproducible and novel method to assess fibrosis.[2,22–25] However, cardiac MR typically requires long examination periods (45 minutes to 1 hour) and is not feasible for all patients. In addition, whole-heart ECV by cardiac MR requires 18–20 breath holds which is time consuming and prohibitive. Thus, an alternative cardiac CT method is highly desirable and may have wide application if shown to be consistent and reproducible.

Cardiac CT is rapidly evolving and has already gained acceptance in certain settings for the evaluation of coronary artery disease.[8,17,26,27] Cardiac CT is tolerated by more patients than cardiac MR, and scan times are typically 10–15 minutes for cardiac CT. An important issue for cardiac CT is radiation dose.[18] The method we have described is equivalent to adding an additional calcium scan to the overall cardiac CT acquisition. Calcium scans generally have a low radiation dose compared with coronary imaging by CT. In this study, the radiation dose for the delayed scan used to assess ECV was 1.9 mSv.

Fibrosis is one of the main features of chronic tissue damage in heart disease. Delayed enhancement cardiac MR is optimized for focal scar detection and is thus insensitive to interstitial fibrosis that is diffuse or mild in degree.[28] Iles et al[5] showed that fibrosis marker correlates well with markers of systolic and diastolic function and with histologically determined collagen content. In this study, decreased myocardial systolic function parameters were associated with increased ECV. Measures of diastolic function as peak filling rate and diastolic volume recovery were not associated with ECV, perhaps because of the small sample size and pseudo-normalization of these diastolic function values.

This study has several limitations. First, cardiac CT ECV validation was based on cardiac MR rather than histologic specimens. Unfortunately, subjects in this study were not eligible for tissue biopsy. However, previous studies have shown consistent histologic correlation between cardiac MR-derived values in both human and animal studies.[5,23,24,29] Second, *regional* variation in ECV may potentially be measureable by this method. Regional evaluation is potentially highly relevant to fibrosis related to coronary artery disease, as well as cardiomyopathies that express regional variations in tissue damage. We have not yet performed region-by-region analysis of ECV values.

NIH-PA Author Manuscript

NIH-PA Author Manuscript

NIH-PA Author Manuscript

5. Conclusion

3D ECV by cardiac CT can be performed with the ECVTK. This toolkit not only facilitates the ECV analysis, but also makes ECV analysis reproducible. We demonstrated increased ECV in subjects with systolic heart failure compared with healthy subjects. Cardiac CT results also showed good correlation with important functional heart biomarkers, suggesting the potential for myocardial tissue characterization with the use of 3D ECV by cardiac CT.

Acknowledgments

Funded by the National Institutes of Health (NIH) Intramural program.

References

1. Mewton N, Liu CY, Croisille P, Bluemke D, Lima JA. Assessment of myocardial fibrosis with cardiovascular magnetic resonance. J Am Coll Cardiol. 2011; 57:891–903. [PubMed: 21329834]
2. Ugander M, Oki AJ, Hsu LY, Kellman P, Greiser A, Aletras AH, Sibley CT, Chen MY, Bandettini WP, Arai AE. Extracellular volume imaging by magnetic resonance imaging provides insights into overt and sub-clinical myocardial pathology. Eur Heart J. 2012; 33:1268–1278. [PubMed: 22279111]
3. Lee JJ, Liu S, Nacif MS, Ugander M, Kawel N, Sibley CT, Kellman P, Arai A, Bluemke DA. Myocardial T1 and extracellular volume fraction mapping at 3 tesla. J Cardiovasc Magn Reson. 2011; 13:75. [PubMed: 22123333]
4. Nacif MS, Kawel N, Sibley CT, Zavodni A, Lima JAC, Bluemke DA. Which is your diagnosis? Radiologia Brasileira. 2011; 44:XI–XIII.
5. Iles L, Pfluger H, Phrommintikul A, Cherayath J, Aksit P, Gupta SN, Kaye DM, Taylor AJ. Evaluation of diffuse myocardial fibrosis in heart failure with cardiac magnetic resonance contrast-enhanced T1 mapping. J Am Coll Cardiol. 2008; 52:1574–1580. [PubMed: 19007595]
6. Nacif MS, Turkbey EB, Gai N, Nazarian S, van der Geest RJ, Noureldin RA, Sibley CT, Ugander M, Liu S, Arai AE, Lima JA, Bluemke DA. Myocardial T1 mapping with MRI: Comparison of look-locker and MOLLI sequences. J Magn Reson Imaging. 2011; 34:1367–1373. [PubMed: 21954119]
7. Senra T, Shiozaki AA, Salemi VM, Rochitte CE. Delayed enhancement by multidetector computed tomography in endomyocardial fibrosis. Eur Heart J. 2008; 29:347. [PubMed: 17827498]
8. Bauer RW, Kerl JM, Fischer N, Burkhard T, Larson MC, Ackermann H, Vogl TJ. Dual-energy CT for the assessment of chronic myocardial infarction in patients with chronic coronary artery disease: comparison with 3-T MRI. AJR Am J Roentgenol. 2010; 195:639–646. [PubMed: 20729440]
9. Siemers PT, Higgins CB, Schmidt W, Ashburn W, Hagan P. Detection, quantitation and contrast enhancement of myocardial infarction utilizing computerized axial tomography: comparison with histochemical staining and 99mtc-pyrophosphate imaging. Invest Radiol. 1978; 13:103–109. [PubMed: 77854]
10. Cury RC, Magalhaes TA, Borges AC, Shiozaki AA, Lemos PA, Junior JS, Meneghetti JC, Rochitte CE. Dipyridamole stress and rest myocardial perfusion by 64-detector row computed tomography in patients with suspected coronary artery disease. Am J Cardiol. 2010; 106:310–315. [PubMed: 20643238]
11. George RT, Silva C, Cordeiro MA, DiPaula A, Thompson DR, McCarthy WF, Ichihara T, Lima JA, Lardo AC. Multidetector computed tomography myocardial perfusion imaging during adenosine stress. J Am Coll Cardiol. 2006; 48:153–160. [PubMed: 16814661]
12. Nacif MS, Kawel N, Lee JJ, Chen X, Yao J, Zavodni A, Sibley CT, Lima JA, Liu S, Bluemke DA. Interstitial myocardial fibrosis assessed as extracellular volume fraction by low radiation dose cardiac ct. Radiology. 2012; 264:876–883. [PubMed: 22771879]

NIH-PA Author Manuscript

NIH-PA Author Manuscript

NIH-PA Author Manuscript

13. Chen X, Nacif MS, Liu S, Sibley C, Summers RM, Bluemke DA, Yao J. A framework of whole heart extracellular volume fraction estimation for low-dose cardiac CT images. IEEE Trans Inf Technol Biomed. 2012; 16:842–851. [PubMed: 22711778]
14. Liu Y, Nacif MS, Liu S, Sibley CT, Bluemke DA, Summers RM, Yao J. Point-guided modeling and segmentation of myocardium for low dose cardiac CT images. IEEE EMBC. 2012:5327–5330.
15. Fernandes VR, Cheng S, Cheng YJ, Rosen B, Agarwal S, McClelland RL, Bluemke DA, Lima JA. Racial and ethnic differences in subclinical myocardial function: the multi-ethnic study of atherosclerosis. Heart. 2011; 97:405–410. [PubMed: 21258000]
16. Kellman P, Arai AE, McVeigh ER, Aletras AH. Phase-sensitive inversion recovery for detecting myocardial infarction using gadolinium-delayed hyperenhancement. Magn Reson Med. 2002; 47:372–383. [PubMed: 11810682]
17. van der Bijl N, de Bruin PW, Geleijns J, Bax JJ, Schuijf JD, de Roos A, Kroft LJ. Assessment of coronary artery calcium by using volumetric 320-row multi-detector computed tomography: comparison of 0.5 mm with 3.0 mm slice reconstructions. Int J Cardiovasc Imaging. 2010; 26:473–482. [PubMed: 20072817]
18. Hausleiter J, Meyer T, Hermann F, Hadamitzky M, Krebs M, Gerber TC, McCollough C, Martinoff S, Kastrati A, Schomig A, Achenbach S. Estimated radiation dose associated with cardiac ct angiography. JAMA. 2009; 301:500–507. [PubMed: 19190314]
19. Young AA, Cowan BR, Thrupp SF, Hedley WJ, Dell'Italia LJ. Left ventricular mass and volume: fast calculation with guide-point modeling on mr images. Radiology. 2000; 216:597–602. [PubMed: 10924592]
20. Osman NF, Prince JL. Regenerating mr tagged images using harmonic phase (harp) methods. IEEE Trans Biomed Eng. 2004; 51:1428–1433. [PubMed: 15311829]
21. Budoff MJ, Nasir K, McClelland RL, Detrano R, Wong N, Blumenthal RS, Kondos G, Kronmal RA. Coronary calcium predicts events better with absolute calcium scores than age-sex-race/ethnicity percentiles: Mesa (multi-ethnic study of atherosclerosis). J Am Coll Cardiol. 2009; 53:345–352. [PubMed: 19161884]
22. Diesbourg LD, Prato FS, Wisenberg G, Drost DJ, Marshall TP, Carroll SE, O'Neill B. Quantification of myocardial blood flow and extracellular volumes using a bolus injection of Gd-DTPA: kinetic modeling in canine ischemic disease. Magn Reson Med. 1992; 23:239–253. [PubMed: 1549039]
23. Lima JA, Judd RM, Bazille A, Schulman SP, Atalar E, Zerhouni EA. Regional heterogeneity of human myocardial infarcts demonstrated by contrast-enhanced MRI. Potential mechanisms. Circulation. 1995; 92:1117–1125. [PubMed: 7648655]
24. Arheden H, Saeed M, Higgins CB, Gao DW, Bremerich J, Wyttenbach R, Dae MW, Wendland MF. Measurement of the distribution volume of gadopentetate dimeglumine at echo-planar MR imaging to quantify myocardial infarction: comparison with 99mTc-DTPA autoradiography in rats. Radiology. 1999; 211:698–708. [PubMed: 10352594]
25. Sibley C, Huang J, Ugander M, Oki A, Han J, Nacif M, Greiser A, Messroghli D, Kellman P, Arai A, Bluemke D, Liu S. Myocardial and blood T1 quantification in normal volunteers at 3t. J Cardiovasc Magn Reson. 2011; 13:P51.
26. Magalhaes TA, Cury RC, Pereira AC, de Moreira VM, Lemos PA, Kalil-Filho R, Rochitte CE. Additional value of dipyridamole stress myocardial perfusion by 64-row computed tomography in patients with coronary stents. J Cardiovasc Comput Tomogr. 2011; 5:449–458. [PubMed: 22146504]
27. Cury RC, Magalhaes TA, Paladino AT, Shiozaki AA, Perini M, Senra T, Lemos PA, Rochitte CE. Dipyridamole stress and rest transmural myocardial perfusion ratio evaluation by 64 detector-row computed tomography. J Cardiovasc Comput Tomogr. 2011; 5:443–448. [PubMed: 22146503]
28. Friedrich MG. There is more than shape and function. J Am Coll Cardiol. 2008; 52:1581–1583. [PubMed: 19007596]
29. Flett AS, Hayward MP, Ashworth MT, Hansen MS, Taylor AM, Elliott PM, McGregor C, Moon JC. Equilibrium contrast cardiovascular magnetic resonance for the measurement of diffuse

myocardial fibrosis: preliminary validation in humans. Circulation. 2010; 122:138–144. [PubMed: 20585010]

NIH-PA Author Manuscript

NIH-PA Author Manuscript

NIH-PA Author Manuscript

NIH-PA Author Manuscript
NIH-PA Author Manuscript
NIH-PA Author Manuscript

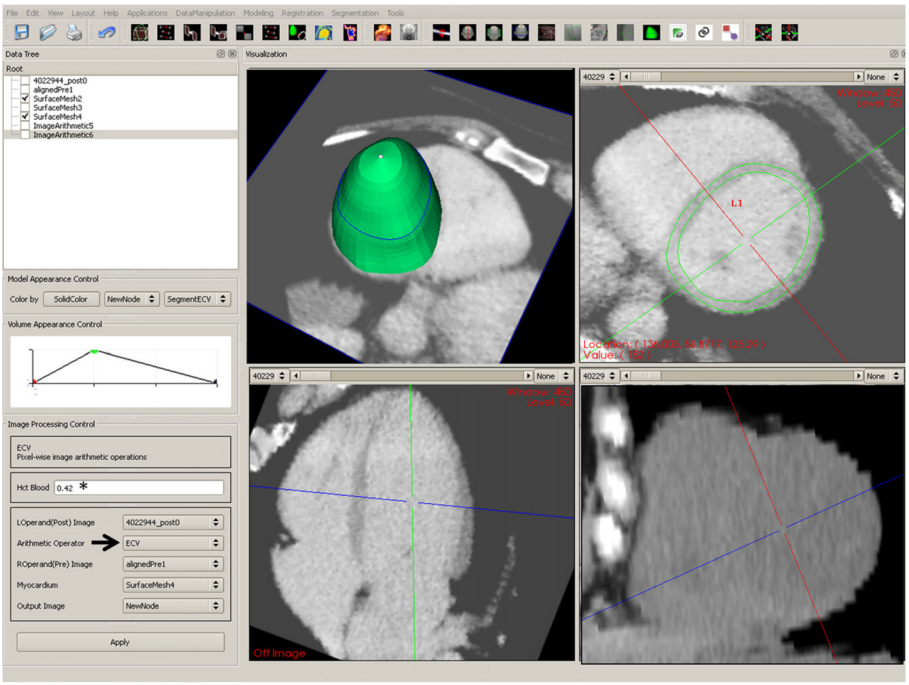

Figure 1.

A screen shot of the extracellular volume (ECV) calculation toolkit (ECVTK). The segmented left ventricle (*top*, *middle*) is shown in green. The volume is derived from segmentation and axial orientation in the short-axis and long-axis views.

NIH-PA Author Manuscript

NIH-PA Author Manuscript

NIH-PA Author Manuscript

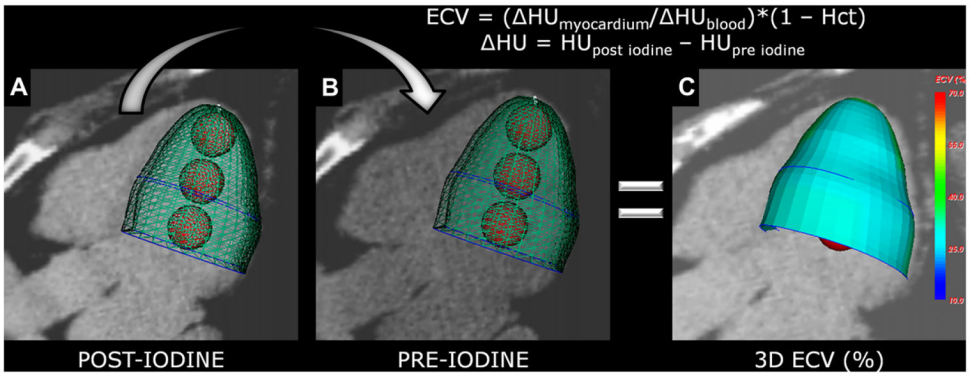

Figure 2.

Calculation of the 3-dimensional (3D) extracellular volume (ECV) map. (A) 3D modeling after iodine for mean measurements of myocardium (*green mesh*) and blood pool (*red balls*) densities (in HU). (B) Same mesh is used to extract myocardium and blood pool densities (in HU) from the data set before -iodine, after image registration. (C) The software automatically calculates mean ECV for each segment and then maps the mean ECV onto the 3D model. Hct, hematocrit.

NIH-PA Author Manuscript

NIH-PA Author Manuscript

NIH-PA Author Manuscript

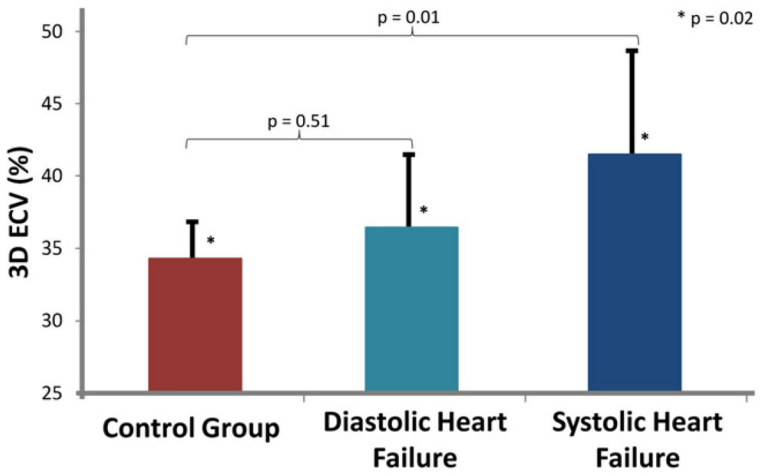

Figure 3.

Discrimination between the healthy and heart failure groups with the use of 3-dimensional (3D) extracellular volume (ECV) by cardiac CT. The healthy and heart failure groups had significantly different mean ECV values ($P = 0.02$). The small vertical lines represent SD of the mean values for ECV.

NIH-PA Author Manuscript
NIH-PA Author Manuscript
NIH-PA Author Manuscript

Table 1

Participant characteristics.

Demographics	Control group (n = 9)	Subjects with diastolic heart failure (n = 5)	Subjects with systolic heart failure (n = 10)	*P* value
Age, y, mean ± SD	59 ± 7	56 ± 20	60 ± 17	0.85
Male, n (%)	4 (44)	2 (40)	5 (50)	0.93
BMI, kg/m^2, mean ± SD	27 ± 3	26 ± 2	27 ± 5	0.76
Hematocrit, %, mean ± SD	41 ± 2	42 ± 1	42 ± 2	0.73
Heart rate, beats/min, mean ± SD	57 ± 3	66 ± 14	65 ± 9	0.10
Serum creatinine, mg/dL, mean ± SD	0.8 ± 0.15	0.8 ± 0.17	0.9 ± 0.15	0.46
NYHA functional class, n II/III (%)	0 (0)	3/2 (60/40)	5/5 (50/50)	NA
Systolic blood pressure, mm Hg, mean ± SD	146 ± 20	128 ± 24	129 ± 20	0.20
Diastolic blood pressure, mm Hg, mean ± SD	69 ± 12	78 ± 9	78 ± 10	0.23
Medical history				
Diabetes mellitus, n (%)	0 (0)	0 (0)	0 (0)	NA
Smoking, n (%)	8 (89)	2 (40)	4 (40)	0.14
Hypertension, n (%)	2 (22)	3 (60)	5 (50)	0.27
Hyperlipidemia, n (%)	4 (44)	2 (40)	2 (20)	0.73
LV systolic function by cardiac MR				
EDV, mL, mean ± SD	145 ± 37	141 ± 24	234 ± 96	**0.02**
ESV, mL, mean ± SD	53 ± 18	60 ± 35	163 ± 75	<**0.001**
EF, %, mean ± SD	63 ± 6	60 ± 12	31 ± 6	<**0.001**
Mass, g, mean ± SD	141 ± 48	111 ± 24	233 ± 84	<**0.01**
Ecc, %, mean ± SD	−19 ± 2	−15 ± 2	−4 ± 3	<**0.001**
LV diastolic function by cardiac MR				
PFR, mL/s, mean ± SD	233 ± 71	262 ± 50	286 ± 124	0.56
TPFR, milliseconds, mean ± SD	623 ± 203	562 ± 20	565 ± 137	0.78
DVR, milliseconds, mean ± SD	880 ± 112	872 ± 115	770 ± 211	0.45
LGE by cardiac MR				
Positive, n (%)	0 (0)	1 (20)	2 (20)	0.39
Coronary calcium by cardiac CT				
Agatston score*, mean ± SD	1.6 ± 0.4	2.0 ± 0.08	1.3 ± 1.2	0.73

BMI, body mass index, calculated as weight in kg/height in m^2; DVR, diastolic volume recovery; Ecc, peak systolic strain rate; EDV, end-diastolic volume; EF, ejection fraction; ESV, end-systolic volume; LGE, late gadolinium enhancement; LV, left ventricular; MR, magnetic resonance; NA, not applicable; NYHA, New York Heart Association; PFR, peak filling rate; TPFR, time to PFR.

*Results from a logistic regression analysis.

NIH-PA Author Manuscript
NIH-PA Author Manuscript
NIH-PA Author Manuscript

Table 2

Myocardial, blood pool, and 3D ECV values.

Parameters	Healthy group (n = 9)	Subjects with diastolic heart failure (n = 5)	Subjects with systolic heart failure (n = 10)	*P* value
Before contrast				
Myocardium, HU, mean ± SD	44.0 ± 5.2	43.0 ± 4.7	38.1 ± 10.9	0.27
Blood pool, HU, mean ± SD	43.2 ± 3.4	46.5 ± 4.5	41.3 ± 8.7	0.34
After contrast				
Myocardium, HU, mean ± SD	82.6 ± 14.2	97.9 ± 5.1	90.3 ± 18.4	0.20
Blood pool, HU, mean ± SD	110.0 ± 22.38	136.5 ± 11.0	117.25 ± 30.5	0.18
ECV				
3D ECV, %, mean ± SD	33.8 ± 2.6*,†	35.7 ± 5.8†	40.8 ± 6.8*	0.02

3D, 3-dimensional; ECV, extracellular volume fraction.

*After post hoc Bonferroni correction, 3D ECV of patients with systolic heart failure was significantly greater than that of control subjects (P = 0.01).

†The 3D ECV of patients with diastolic heart failure was not significantly different than that of control subjects (P = 0.51).

NIH-PA Author Manuscript
NIH-PA Author Manuscript
NIH-PA Author Manuscript

Table 3

3D ECV by cardiac CT versus clinical and imaging parameters.

Parameter	Correlation coefficient, 3D ECV by cardiac CT	*P* value*
Age	0.13	0.61
Male	0.20	0.43
BMI	0.03	0.89
Hematocrit (%)	0.30	0.20
Heart rate (beats/min)	0.50	0.04
Serum creatinine (mg/dL)	0.009	0.97
Systolic blood pressure (mm Hg)	0.32	0.19
Diastolic blood pressure (mm Hg)	0.02	0.95
Smoking	0.21	0.40
Hypertension	0.10	0.68
Hyperlipidemia	0.42	0.07
EDV (mL)	0.60	<0.001
ESV (mL)	0.74	<0.001
EF (%)	0.68	<0.001
Mass (g)	0.32	0.19
Ecc (%)	0.71	<0.001
PFR (mL/s)	0.18	0.48
TPFR (millisecond)	0.20	0.44
DVR (millisecond)	0.43	0.10
Agatston score†	0.43	0.06

3D, 3-dimensional; BMI, body mass index, calculated as weight in kg/height in m^2; DVR, diastolic volume recovery; Ecc, peak systolic strain rate; ECV, extracellular volume fraction; EDV, end-diastolic volume; EF, ejection fraction; ESV, end-systolic volume; PFR, peak filling rate; TPFR, time to PFR.

**P* value, for linear or logistic regression analysis as appropriate, relating ECV as the dependent variable and the column 1 value as the independent variable.

†Results from a logistic regression analysis.